Electromagnetic Formation Flight

Progress Report: May 2002

Submitted to: Lt. Col. John Comtois
                       Technical Scientific Officer
                       National Reconnaissance Office

Contract Number: NRO-000-02-C0387-CLIN0001

MIT WBS Element: 6893087

Submitted by: Prof. David W. Miller
                       Space Systems Laboratory
                       Massachusetts Institute of Technology

DESCRIPTION OF THE EFFORT

The Massachusetts Institute of Technology Space Systems Lab (SSL) and the Lockheed Martin Advanced Technology Center (ATC) are collaborating to explore the potential for a Electro-Magnetic Formation Flight (EMFF) system applicable to Earth-orbiting satellites flying in close formation.

PROGRESS OVERVIEW

At MIT, work on electro-magnetic formation flight (EMFF) has been pursued on two fronts: the MIT conceive, design, implement and operate (CDIO) class, and the MIT Space Systems Lab research group, as described in the April 2002 progress report.

The CDIO class has just completed its first semester performing trades on and preliminary design of a six-degree-of-freedom electromagnetic formation flight testbed, called "ElectroMagnetic Formation Flight of Rotating Clustered Entities," or "EMFFORCE." EMFFORCE will utilize electromagnets to control the size and attitude of a cluster of bodies. The MIT Space Systems Lab research staff is supporting the CDIO class with both hardware and software analysis and design.

Recent work has focused on the design and analysis of a control system for the EMFFORCE testbed. Specifically, three testbed modes have been considered:

- **Spin-up** of multiple bodies from rest
- **Steady-state spin** of multiple bodies, ensuring:
    – Operation at a fixed cluster radius
    – Disturbance rejection
- **Spin-down** of multiple bodies from steady-state spin.

Analysis shows the steady-state spin mode to be unstable, yet controllable with either simple PID control or more optimal state-space control methods. Further, a one-degree-of-freedom air-track system is identified to have unstable dynamics almost identical to the dynamics of a spinning cluster; hence demonstrating control on the air track system will be considered a positive step toward demonstrating control on the spinning system.

The following report summarizes recent progress on the control analysis and design for the first two configurations. The third configuration will be treated similarly to the first, but with a "reversed" algorithm.

Preliminary Control Design For the "Electromagnetic Formation Flight of Rotating Clustered Entities" (EMFFORCE) Testbed in the MIT Space Systems Laboratory

1 Subsystem Overview
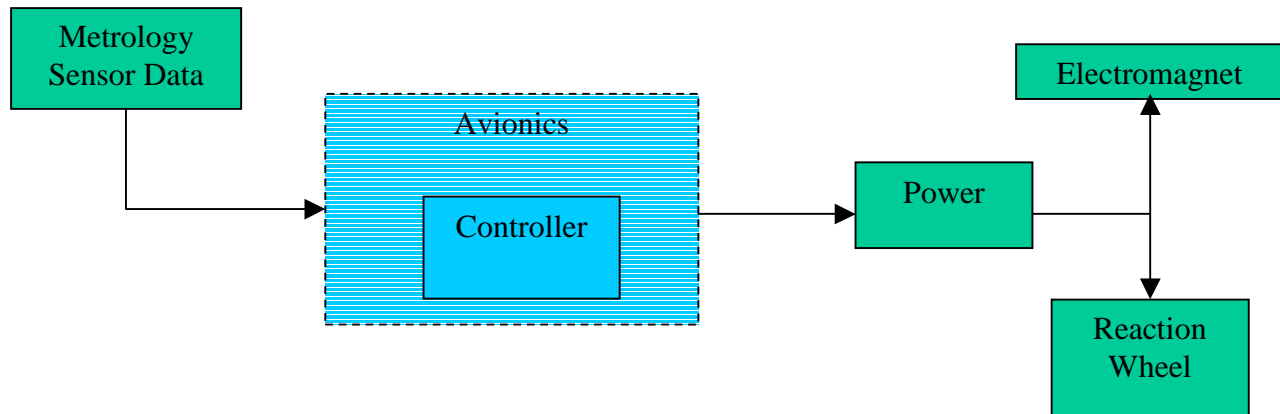
Figure 1.1 Control Subsystem Flow Chart

The control subsystem, a computer program located within the avionics processor, takes state inputs from the metrology subsystem and compares the current state with the desired state. It then outputs commands, in the form of an output voltage, to the actuators to adjust the current state to match the desired one. The output voltages are fed through the power system, which powers the actuators.
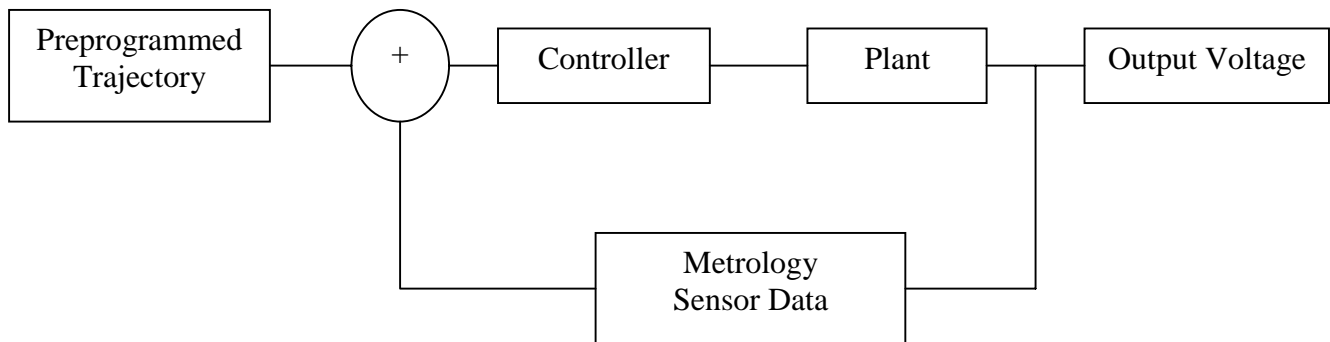
Figure 1.2 Feedback System

There are two different actuators to control the system, the electromagnets and the reaction wheels. The electromagnets can provide forces and torques along the three degrees of freedom in which the vehicles operate (x, y, and θ). Unfortunately, since the forces produced by the electromagnet cannot be independently controlled, there is also need for a reaction wheel. The reaction wheel produces a torque

about the θ axis and it provides the opportunity to place the electromagnet's magnetic poles. It is with these two actuators that all controlling forces will be produced.

The requirements for the controller are derived from the requirements document. The main requirement is to create a robust controller. This implies both rejecting any disturbance force that the formation may encounter and having enough control authority to reposition satellites within the formation.

To demonstrate a robust controller, the system must execute three maneuvers: spin-up, steady state spin, and spin-down. The spin-up maneuver consists of controlling three vehicles initially at rest in a straight line with perpendicular magnetic fields (See Figure 1.3) to follow a specified trajectory to the steady state configuration. In steady state spin the cluster is spinning about the center vehicle with an angular rotation rate of at least 1 RPM. This configuration has all three magnetic fields lined up along a common axis. Spin-down follows the same trajectory as spin-up in reverse. From the steady state the system will gradually cause its magnetic fields to be perpendicular so as to stop the clusters motion. These maneuvers are further developed in Sections 2 and 3.
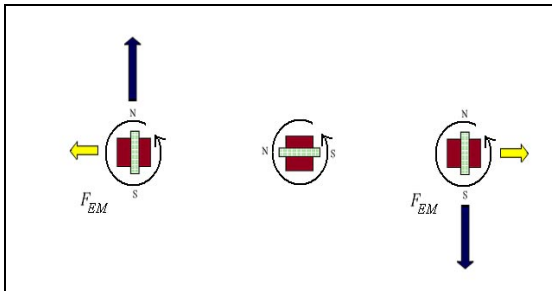
Figure 1.3 Three Vehicle Spin-Up   **Figure 1.4 Three Vehicle Steady State**
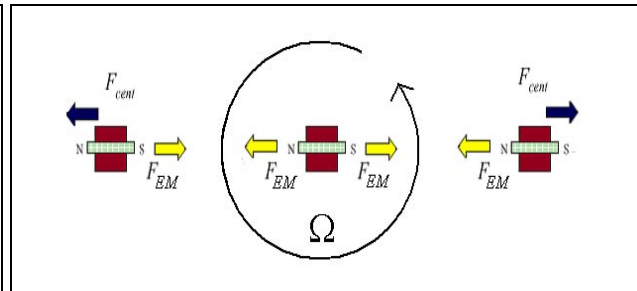
The last requirement determines the control tolerance. Derived from the accuracy of our analysis, the maximum displacement error allowed is one tenth of the separation distance between two adjacent vehicles. For the specified maneuver, the maximum displacement error should not exceed 20 cm.

2 Steady State Mode

2.1 Definition of Steady State Mode

After the vehicles have completed the spin-up maneuver, they should complete three revolutions in steady state mode. The steady state mode defines the control algorithm for this system maneuver. The steady state mode will seek to decrease the error between the desired separation distance and the actual separation distance. Since the purpose of the steady state mode is to keep the vehicles in configuration, this controller will mostly reject disturbances. To design a controller, the system must first be analyzed. Since the force from the electromagnets is axial then it is necessary to analyze the axial dynamics of the system.

First, a system model must be developed. Force balance and perturbation analyses are used to find the dominant poles of the system. In this mode, the forces acting on the system are the electromagnetic forces from each electromagnet, and the centripetal force due to rotation. For a configuration with three vehicles where the magnetic moments are $\mu_A = \mu_B = \mu_C = \mu_{avg}$, the forces are:

$$F_{cent.} = \frac{mv^2}{s} = m\Omega^2 s = \frac{mh^2}{s^3}, \quad F_{EM} = \frac{c_0\mu_{avg}^2}{s^4} + \frac{c_0\mu_{avg}^2}{(2s)^4}$$

Equation 2.1 Centripetal and Electromagnetic Forces Used in Steady-State Force Balance

where Ω is the angular rotation of the system and s is the separation distance from the middle vehicle to the outer vehicles and h is the angular momentum of the cluster per unit mass.
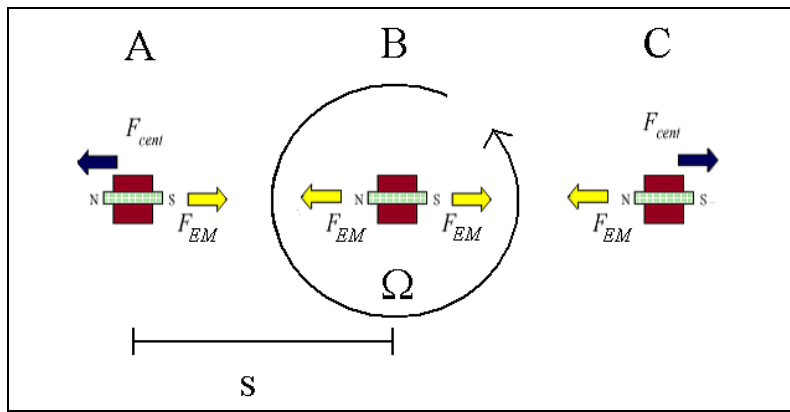
Figure 2.1 Three Vehicle Steady State Force Balance

The difference of these forces produces acceleration of the vehicles. A perturbation is then added to the equation.

$$m(\ddot{s}_0 + \delta\ddot{s}) = \frac{mh^2}{(s_0 + \delta s)^3} - \frac{17c_0(\mu_{avg} + \delta\mu_{avg})^2}{16(s_0 + \delta s)^4}$$

Equation 2.2 Perturbation Analysis

Using binomial expansion and neglecting the higher order terms, the equation simplifies to

$$m\delta\ddot{s} - \frac{mh^2}{s_0^4}\delta s = -2\frac{mh^2}{\mu_{avg}s_0^4}\delta\mu$$

Equation 2.3 Simplified Equation of Motion

Taking the Laplace transform of the equation of motion, the homogeneous solution indicates the poles are at plus and minus Ω on the real axis. With this analysis, carried out in great detail in Appendix A, it is determined that steady state spin is unstable with a pole in the right half plane. A controller can, however, be designed to stabilize the system based on this model.

2.2   Discussion of Trades Analysis

Different approaches can be used to design the controller to stabilize the steady state mode. Two different control approaches were explored, phase lead and state space.

2.2.1 Phase Lead Controller

One approach is a phase lead control. A pair of students, Farmey Joseph and Richard Cross, in MIT's Aeronautical and Astronautical department's junior design project class, 16.62x, explored a system with a similar model as the steady state mode model found above, and implemented a phase lead controller to stabilize the system. Their work was performed under the guidance of Professor David W. Miller in the MIT Space Systems Laboratory.

Their setup consisted of a linear air track and two magnets. Originally, both magnets were to be electromagnets that would glide on the air track and be controlled through current regulation. Due to a miscalculation, the electromagnetic forces produced were not strong enough to demonstrate control. Therefore, the free magnet was replaced with a permanent magnet.

With the 16.62x system, there are two different possible setups, one stable and one unstable. The 16.62x students examined the stable setup, in which the air track is raised on one end and the electromagnet is fixed at the other end. The electromagnet must repel the permanent magnet to maintain a fixed separation distance. The arrows indicate the direction of the magnets' north poles.
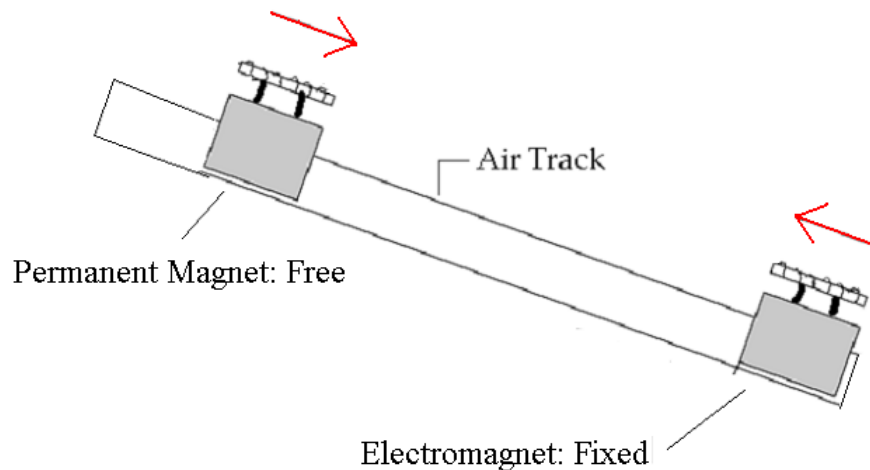
Figure 2.2 16.62x Stable Setup

The stable system is modeled in Appendix A.2.1. The dominant system poles are found to be at $\pm\sqrt{\dfrac{6\mu_0\mu_{avg}^2}{\pi s_0^5 m}}i$, with a root locus on the imaginary axis. The 16.62x students located the poles

by taking a step response of the system, which depicts the lack of damping in the uncontrolled system.
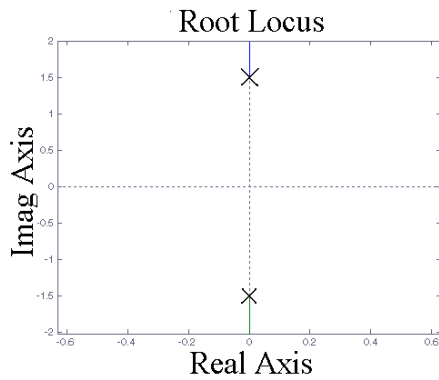
Figure 2.3 Root Locus of the Stable System   **Figure 2.4 Uncontrolled Step Response**
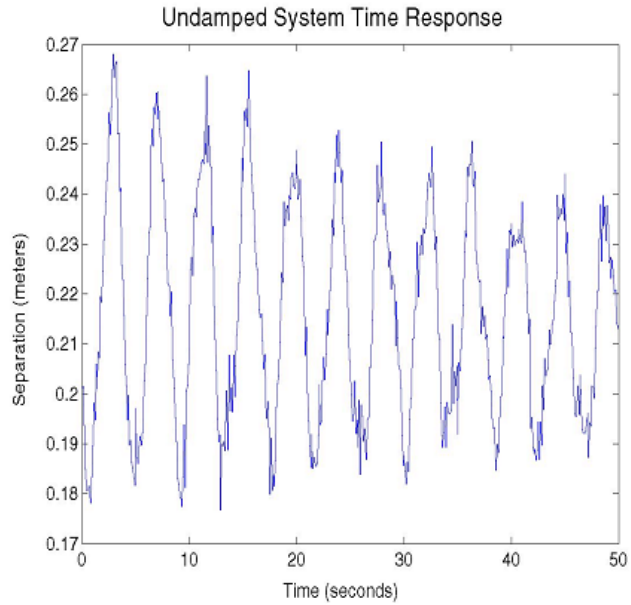
The actual poles were found to be at plus and minus 1.5i. A phase lead controller was implemented with a pole at -20, a zero at -2, and a gain of 0.5. This effectively reduced the oscillations of the system when a step was introduced. The controller provided a damping ratio of 0.11. There was some error, however, which was due to sensor noise.
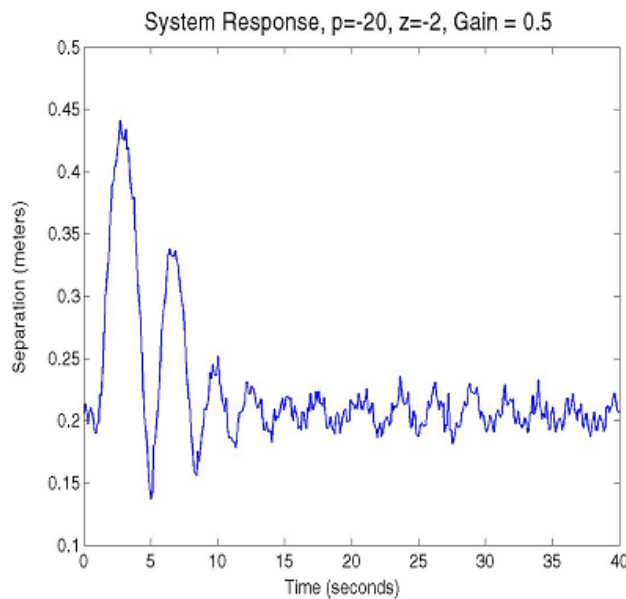
Figure 2.5 Controlled Step Response of Stable Setup

Another possible setup with the linear air track demonstrates the unstable case. To create this setup, the air track is raised on the same side as the fixed electromagnet. To maintain a fixed separation distance, the fixed electromagnet must attract the free permanent magnet to maintain a fixed separation distance.
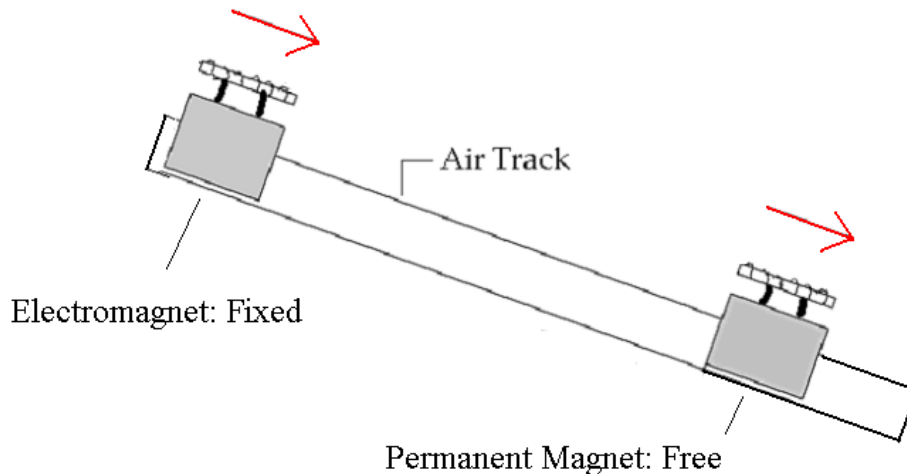
Figure 2.6 16.62x Unstable Setup

The unstable setup is modeled in Appendix A.2.2. Like the stable setup, the dominant system poles are found to be at $\pm\sqrt{\dfrac{6\mu_0\mu_{avg}^2}{\pi s_0 m}}$, but on the real axis instead of the imaginary axis. This puts a pole in the right half plane, making the system unstable. In this way, the unstable setup is similar to the steady state mode of the project. Controlling the unstable setup should be similar to controlling the steady state mode.
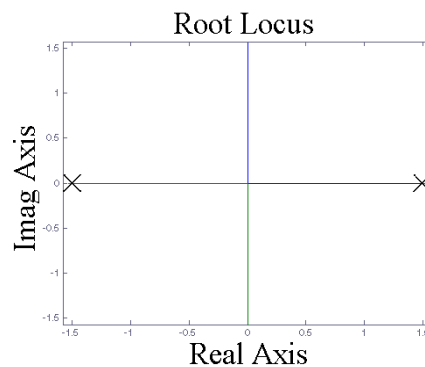
Figure 2.7 Root Locus of Unstable System

The 16.62x students did not implement a controller for the unstable system, so the EMMFORCE controls team designed a controller in SISOTOOL in MATLAB. A phase lead controller, similar to the one used in the stable setup, was used, with a pole at –20, a zero at –3, and a gain of 30. This gives a damping ratio of about 0.68. The step response shows a small steady state error, but

the system stabilizes quickly, within about 1 second. The overshoot is small, with no oscillations. When this controller is implemented on the unstable setup, it should demonstrate control.
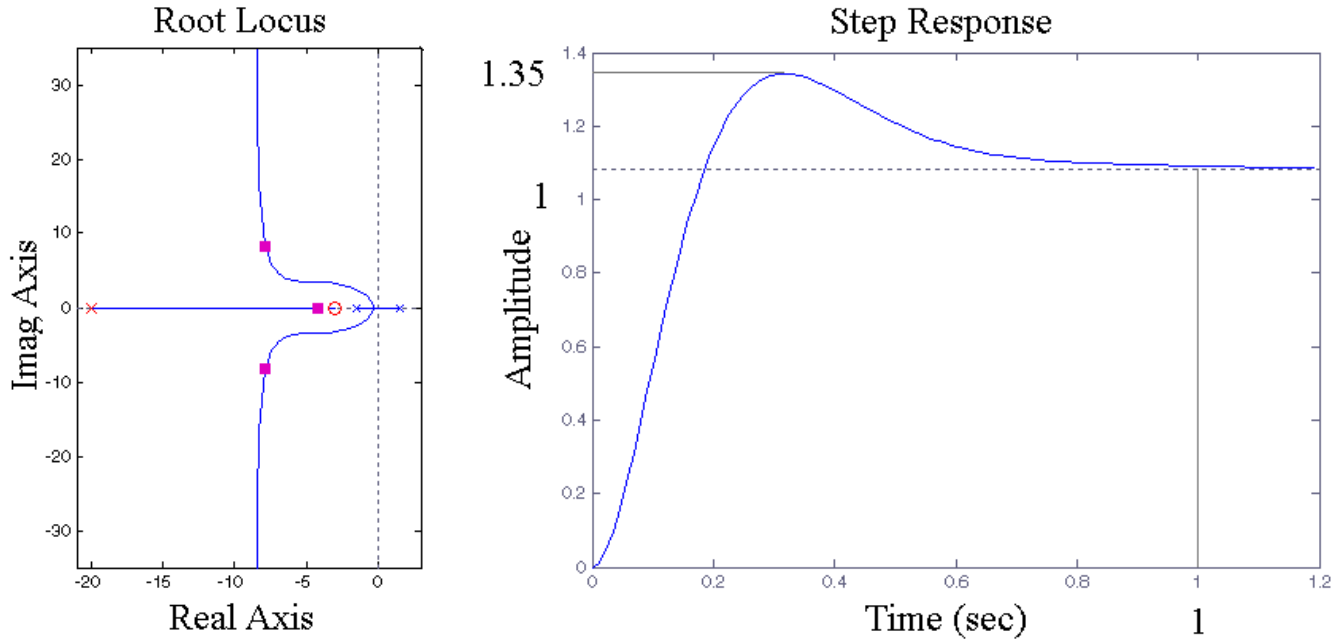
Figure 2.8 Root Locus and Step Response of Controlled System

2.2.2 State Space Analysis

From equation 2.3, the equation of motion, a state space equation can be developed.

$$
\begin{bmatrix} \dfrac{\delta \dot{s}}{s_0} \\[2ex] \dfrac{\delta \ddot{s}}{s_0} \end{bmatrix} = \begin{bmatrix} 0 & 1 \\ \Omega^2 & 0 \end{bmatrix} \begin{bmatrix} \dfrac{\delta s}{s_0} \\[2ex] \dfrac{\delta \dot{s}}{s_0} \end{bmatrix} + \begin{bmatrix} 0 \\ -2\Omega^2 \end{bmatrix} \dfrac{\delta \mu}{\mu_{avg}}
$$

Equation 2.4 State Space Equation of Motion in Form $\dot{x} = Ax + Bu$

Using modern control techniques the closed loop poles for cost efficient controllers can be found. The following derivation is performed in more detail in Appendix A.3. To develop this controller, a cost function is created to weigh the importance of different parameters. R_{xx} is defined as a two by two matrix that allows one to penalize differences in separation or velocity of the vehicles. R_{uu} is a scalar that describes the cost of using control. Because the controller commands power to be supplied to the actuators, controlling the system has a cost of power. The cost function weighs the importance of accuracy in positioning the satellites with the limited resource of power.

$$J = \int_0^\infty [x^T R_{xx} x + u^T R_{uu} u] dt$$

Equation 2.5 Cost Function

Cost is minimized when the following two equations hold.

$$R_{xx} + PA + A^T P - PBR_{uu}^{-1} B^T P = 0$$

Equation 2.6 Equation 1 for Cost Minimization

$$u = -R_{uu}^{-1} B^T P x = -Fx$$

Equation 2.7 Equation 2 for Cost Minimization

Here, the P matrix is an unknown. When P is determined from equation 2.6, it can be substituted into equation 2.7 and the feedback F can be solved. Because displacement is more important for our control than velocity, R_{xx} is given a variable λ in displacement term. R_{uu} is assigned a variable ρ.

$$R_{uu} = \rho \qquad R_{xx} = \begin{bmatrix} \lambda & 0 \\ 0 & 0 \end{bmatrix} \qquad P = \begin{bmatrix} P_{11} & P_{12} \\ P_{12} & P_{22} \end{bmatrix}$$

Equation 2.8 Variable Definitions

As shown in the derivation in Appendix A.3, P can be solved for in terms of λ, ρ, and Ω. With these variables, the most efficient controller can be calculated given a set ration of λ and ρ. If the ratio λ/ρ is evaluated from $0 \rightarrow \infty$, a graph of the closed loop poles for the most efficient controller can be created.
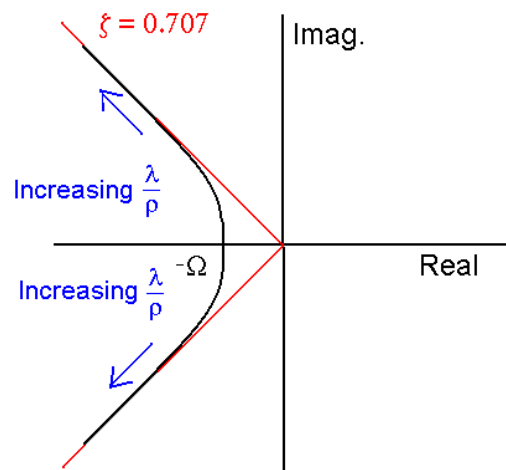
Figure 2.9 Closed Loop Pole Locations for Varying Ratios of λ/ρ

When the ratio is zero, use of control is infinitely expensive and the poles are both located at $-\Omega$. When the ratio is infinity, use of control is infinitely cheap. The location of the closed loop poles move out to infinity along the 45° asymptote, where the damping ratio is 0.707.

2.3 Summary Of Options/Selection Criteria

Both methods of developing a controller provide beneficial information. The phase lead approach will most likely be simpler to calculate and easier to analyze with the current knowledge of the EMFORCE controls team. Though it is more complicated, the state space approach allows greater focus on the important factors of cost and accuracy. For a preliminary control design, the classic control technique of phase lead controllers will be implemented. For a final control design, the state space approach may be used.

3 Spin-up/Spin-down Mode

3.1 Definition of Spin-up/Spin-down

When starting from rest, the vehicles must perform a spin-up maneuver to reach steady state spin. After three steady state revolutions, the vehicles must perform a spin-down maneuver to return to rest. These maneuvers are similar and will be modeled and controlled by similar means. The spin-up/spin-down mode defines the control algorithm for these system maneuvers. This controller will try to move the vehicles, initially at rest, along some pre-defined trajectory to the steady state spin configuration (See Figure 3.1). To design a controller, the system must first be analyzed. Since this mode involves mostly electromagnetic torques and translational forces, these system dynamics must be analyzed.

Initially the three vehicles will be positioned on the test bed at the appropriate separation distances with the magnetic fields perpendicular to each other. The effects of this configuration are that the magnets experience a shearing force, shown in the following figure by straight arrows, and a torque, shown by the curved arrows.
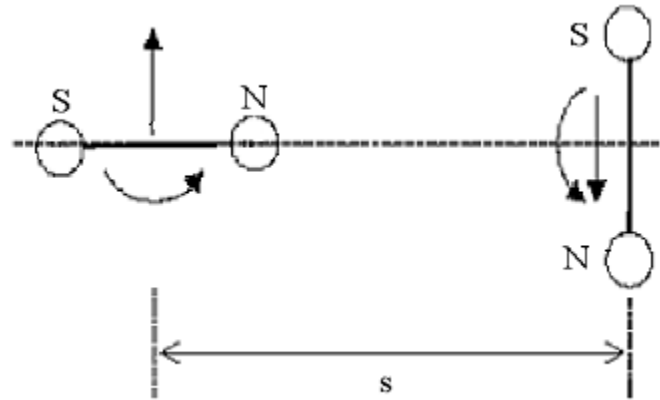
Figure 3.1 Spin-up Force Balance

This figure depicts two vehicles, but the same forces apply with three or more vehicles. When these forces and torques are controlled to follow a specified trajectory, the electromagnets can be caused to move from rest to orbiting about a midpoint. This trajectory, for three vehicles, is depicted below:
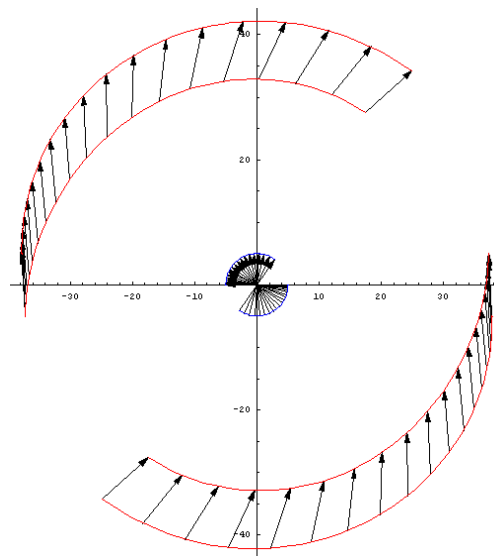
Figure 3.2 Three Vehicle Spin-up Trajectory

When spinning up, the vehicles will experience disturbances. Any number of disturbances can cause one or more vehicles to translate. Therefore it is important to take into account the translational forces of two electromagnets with perpendicular magnetic fields. As shown below, the translated vehicles motion will be governed by a translational force that changes depending on the translated distance. This line of motion is broken into three regimes. If a magnet is disturbed past a critical distance in either direction, then the translational force will change direction.
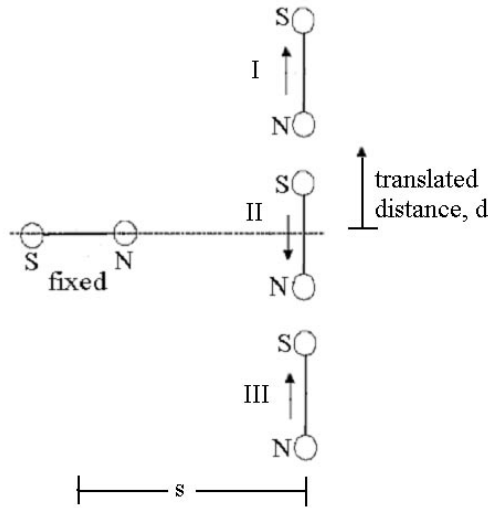
Figure 3.3 Three Regimes of Motion for Spin-up

At the critical points, where the translational forces change direction, the magnitude of the force is zero, making them equilibrium points. To locate the points, the translational force must be calculated for a given displaced distance. The translational force is a function of the angles of each electromagnet's magnetic field to the axis that runs between them. As one magnet becomes more and more displaced these angles change. The angles are defined as follows:
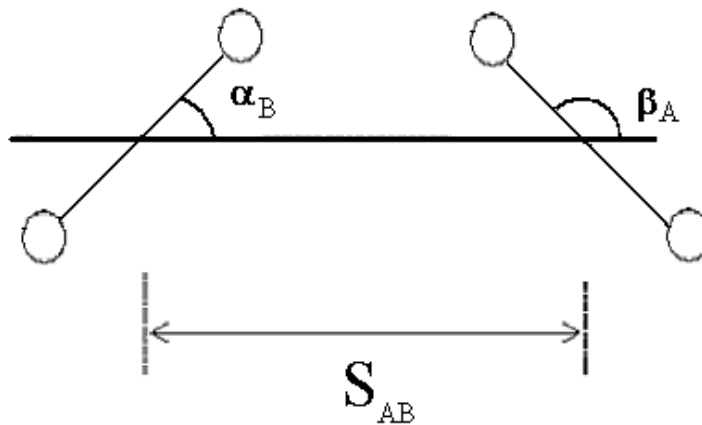
Figure 3.4 Angle Definition

Defining force based on angle,

$$F_{trans} = \frac{3\mu_0\mu_{avg}^2}{4\pi s_{AB}^4}\left[Sin(\alpha_B + \beta_A)\right]$$

Equation 3.1 Translation Force Dependent on Angle

At the equilibrium points, $sin(\alpha_B + \beta_A) = 0$. From the geometry, the equilibrium points occur when the translated distance, d, is equal to the separation distance, s_{AB}. Shown below is a phase plane plot of the movement of the vehicle. This analysis defines the movement of the vehicles in any regime, as shown

below. If near the equilibrium point on the left, the vehicle will oscillate forever. In any other location, the vehicle will move towards infinity.
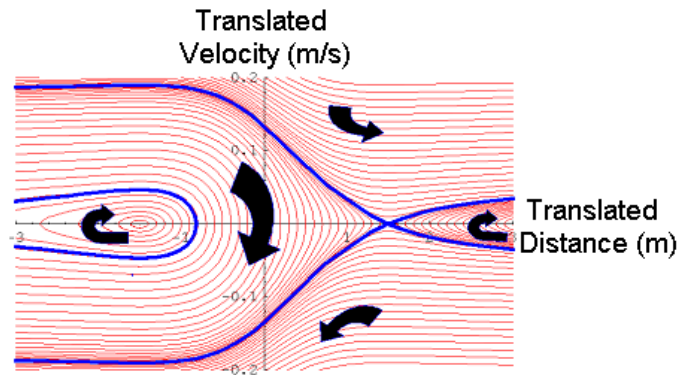
Figure 3.5 Travel Paths for Given Translated Distances

A controller must be designed to follow the given trajectories without leaving the stable regimes.

3.2 Discussion of Trades Analysis

There is a trade between the two possible spin-up configurations.
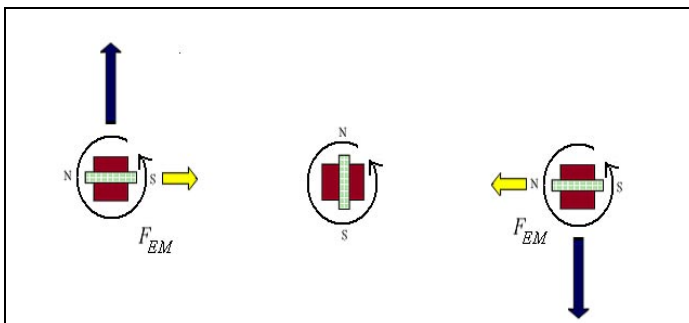
Figure 3.6 Spin-up Configuration 1   **Figure 3.7 Spin-up Configuration 2**
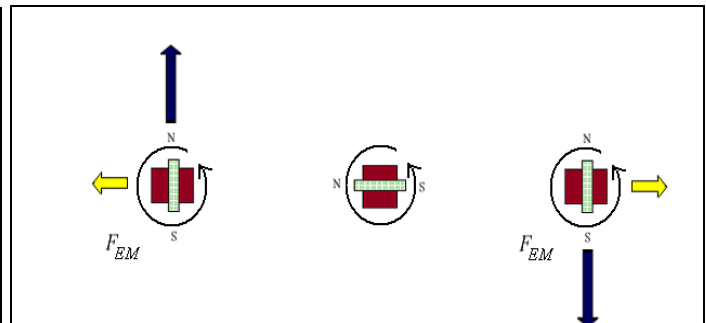
The basis for this trade lies in the fact that the forces and moments on each magnet are not equal. As shown in the following figure, due to the geometry of the configuration -- mainly that the separation distance, s, significantly larger than the half length of the electromagnetic core -- the torques are different on each vehicle.
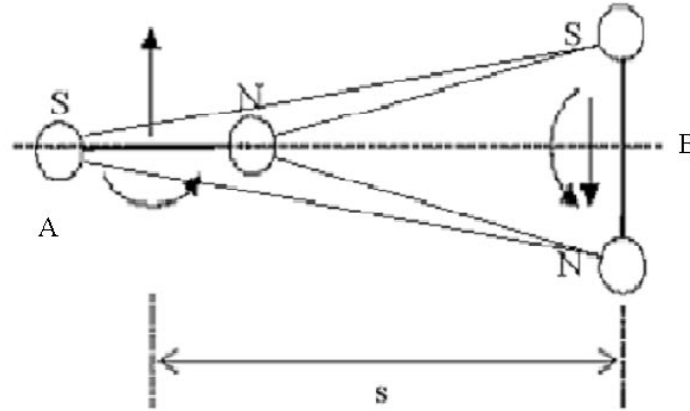
Figure 3.8 Unequal Torques on Vehicles

In this configuration, the torque felt by magnet B is greater than the force felt on magnet A. If a straight-line force between the poles is assumed, it is seen that the angle at which the force reaches the poles on magnet B approaches 90° and the angle at which the force reaches the poles on magnet A is closer to zero. Since torque is the product of the force and the sine of the angle, the torque on magnet B is much greater than the torque on magnet A.

More analytically, the torques on each magnet can be calculated.

$$\tau_A = \frac{\mu_0 \mu_{avg}^2}{8\pi} \left[Sin(\alpha_B - \beta_A) + 3(\alpha_B + \beta_A) \right] \qquad\qquad \tau_B = \frac{\mu_0 \mu_{avg}^2}{8\pi} \left[Sin(\beta_A - \alpha_B) + 3(\beta_A + \alpha_B) \right]$$

Equation 3.2 Torques on Vehicles

When $\alpha_B = 0°$, and $\beta_A = 90°$, the torque on magnet A is half the torque on magnet B.

$$\frac{\tau_A}{\tau_B} = \frac{\dfrac{\mu_0 \mu_{avg}^2}{8\pi} \left[Sin(\alpha_B - \beta_A) + 3(\alpha_B + \beta_A) \right]}{\dfrac{\mu_0 \mu_{avg}^2}{8\pi} \left[Sin(\beta_A - \alpha_B) + 3(\beta_A + \alpha_B) \right]} = \frac{2}{4} = \frac{1}{2}$$

Equation 3.3 Torque Ratio

Because the torques are not equal on each vehicle, there is a trade between the two configurations in figures 3.6 and 3.7.

3.3 Summary of Options/Selection Criteria

Since the torque on the vertically aligned magnets is greater than the torque on the horizontally aligned magnets, it follows that the initial positions of the magnets is important. In the configuration of figure 3.7, the center magnet feels half the torque of the outer one; its torque is then doubled due to the other outer vehicle producing an even distribution of moments among the three vehicles. In figure 3.6, the center magnet feels twice the torque of the outer one, which is then doubled due to the existence of the

other outer vehicle. Therefore, the center magnet feels four times the amount of torque as compared to the outer ones.

The amount of torque on a vehicle determines the amount of counter-torque the reaction wheel will have to exert for control.   If the torque is concentrated in one vehicle then this vehicle will have to have a larger reaction for adequate control. On the other hand, a large center vehicle means that more of the system mass is concentrated at the center leading to less cluster angular momentum thus less total reaction wheel angular momentum. Less reaction wheel angular momentum means that the reaction wheels can be smaller, which affects the electromagnet size. A larger center vehicle also allows for a larger central magnet, therefore a stronger central magnetic field. The result of a larger central magnetic field is that the system can operate with lighter outer vehicles, at greater separation distance, and/or at greater angular velocity. A large center vehicle with smaller outer vehicles, unfortunately violates our interchangeability requirement. This requirement stipulates that all three vehicles must be the same. The interchangeability requirement favors the configuration of figure 3.7, since this configuration more evenly distributes the angular momentum among the three vehicles, leading to the smallest possible reaction wheels, thus lighter-weight vehicles.

Because the requirements must be met, the configuration of figure 3.7 is the feasible configuration. However, if the requirements change, the configuration may change to that of figure 3.6.

4 Control Architecture

4.1 Definition of Control Architecture

The control subsystem must know what mode to control, steady state or spin-up/spin-down. It then must know how to implement the correct control for the determined mode. There are different methods of processing the sensor data and issuing response commands. The control architecture determines the desired trajectory and implements the appropriate controller.   It also determines the manner of communicating the control instructions.

4.2 Discussion of Trades Analysis

The main trade for control architecture is the location of the controller within the entire system.   Three options were analyzed. These were independent, centralized control, and hybrid control.

With independent control, the vehicles each collect and process data to derive a control solution for each separate vehicle. Because each vehicle will be processing and responding to its own data, the response time will be very quick. The main disadvantage, however, of independent control is conflict with multiple vehicles controlling the same disturbance. The system is coupled, therefore, when one vehicle moves, it affects the others. It will be very difficult to implement independent control with each vehicle impacting the state of the others.

In centralized control, all of the information from metrology will be sent to a hub vehicle. The hub would calculate the control solution and send the commands to the other vehicles. This is a good solution to the problem of a coupled system. With only one vehicle making decisions, there is no conflict with vehicles responding to other vehicles. However, there is a significant time delay associated with a centralized controller. Having a hub run calculations and then send commands to other vehicles slows down the response time.

The last form of control is hybrid control. In this case, all three vehicles will possess the ability to control independently. In times when a quick response is needed, independent control will be implemented. The system will also be capable of controlling through a hub vehicle in cases where timing is not as crucial or the coupled effects of using electromagnetic actuation jeopardize adequate control.

4.3 Summary Of Options/Selection Criteria

Neither independent control nor centralized control is very feasible to use separately. The effects of being a coupled system are too large to use only independent control, and response time will most likely not be quick enough if a hub did all of the calculations. Therefore, the best option is to implement a hybrid control system. When timing is crucial, independent control will be implemented. At all other times, a centralized controller will process the data and issue the commands to the other vehicles.

5 External Interfacing Needs

The control subsystem is located within the avionics subsystem. It is programmed onto the avionics processor. In this way, it interfaces with avionics.

The controller will need inputs from metrology of the current state. This will include at least the separation distance, the vehicles relative bearing, and the relative angles of the electromagnets' poles. Other inputs that will not be required, but helpful in implementing control are the velocity and acceleration of the vehicles.

After calculating the control algorithms, the control subsystem will output commands to the power subsystem. These commands will indicate how much power needs to be supplied to the actuators.

6 Conclusions

The control design is central to building a successful system; indeed, it is what this testbed is attempting to show is feasible. Unfortunately the controller design is not straightforward. As has been mentioned, the control problem is unstable and the main actuator, the electromagnet, produces forces and torques that are coupled. Through careful analysis the system's dynamics can become well understood and certain trades can be made leading to possible control designs.

Appendix A

Appendix A.1 Derivation of Poles for Steady State

Force Balance
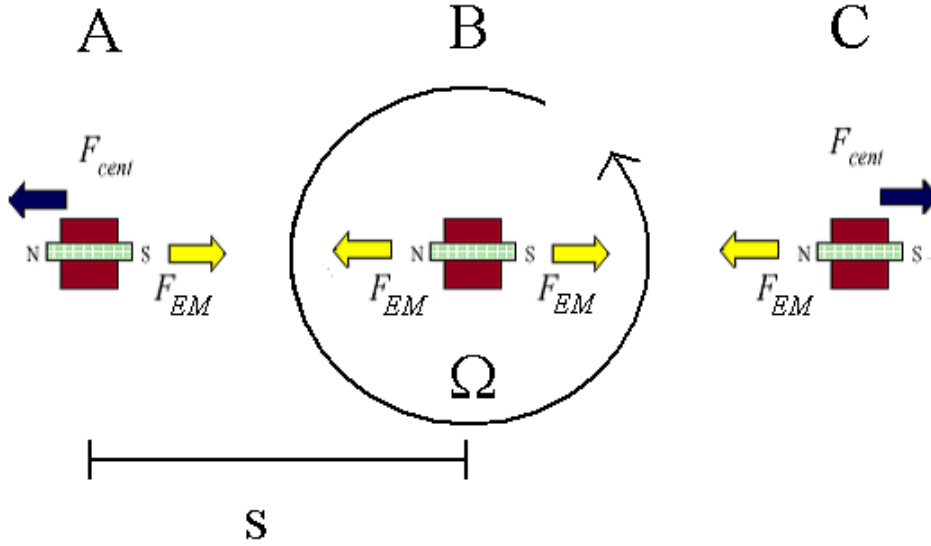
Assume the three vehicles have the same magnetic moments, so $\mu \equiv \mu_A = \mu_B = \mu_C$.

Equation A.1.1 $$F_{cent.} = \frac{mv^2}{s} = m\Omega^2 s = \frac{mh^2}{s^3}$$

Equation A.1.2 $$F_{EM} = \frac{c_0\mu^2}{s^4} + \frac{c_0\mu^2}{(2s)^4} \qquad \text{where} \quad c_0 = \frac{3\mu_0}{2\pi}$$

Equation A.1.3 $$m\ddot{s} = F_{cent.} - F_{EM} = \frac{mh^2}{s^3} - \frac{c_0\mu^2}{s^4} - \frac{c_0\mu^2}{(2s)^4}$$

Add a perturbation

$$m(\ddot{s}_0 + \delta\ddot{s}) = \frac{mh^2}{(s_0 + \delta s)^3} - \frac{17c_0(\mu_{avg} + \delta\mu)^2}{16(s_0 + \delta s)^4}$$

$\ddot{s}_0 = 0$ because s_0 is the constant, steady-state displacement

$$m\delta\ddot{s} = \frac{mh^2}{s_0^3(1 + \frac{\delta s}{s_0})^3} - \frac{17c_0\mu_{avg}^2(1 + \frac{\delta\mu}{\mu_{avg}})^2}{16s_0^4(1 + \frac{\delta s}{s_0})^4}$$

Binomial Expansion $(1+x)^n = 1 + nx +$ higher order terms for $|x| \ll 1$

$$m\delta\ddot{s} = \frac{mh^2(1-3\frac{\delta s}{s_0})}{s_0^3} - \frac{17c_0\mu_{avg}^2(1+2\frac{\delta\mu}{\mu_{avg}})(1-4\frac{\delta s}{s_0})}{16s_0^4}$$

$$m\delta\ddot{s} = \frac{mh^2(1-3\frac{\delta s}{s_0})}{s_0^3} - \frac{17c_0\mu_{avg}^2(1+2\frac{\delta\mu}{\mu_{avg}}-4\frac{\delta s}{s_0}-8\frac{\delta\mu\delta s}{\mu_{avg}s_0})}{16s_0^4}$$

Neglect Higher Order Terms

$$m\delta\ddot{s} = \frac{mh^2(1-3\frac{\delta s}{s_0})}{s_0^3} - \frac{17c_0\mu_{avg}^2(1+2\frac{\delta\mu}{\mu_{avg}}-4\frac{\delta s}{s_0})}{16s_0^4}$$

Cancel Force Balance Terms

In the steady state case, when $\ddot{s} \to 0$ (so that $s = s_0$, and $\mu = \mu_{avg}$):

$$F_{cent.} - F_{EM} = \frac{mh^2}{s_0^3} - \frac{17c_0\mu_{avg}^2}{16s_0^4} = 0$$

so that the steady-state terms cancel in the equation of motion, leaving:

$$m\delta\ddot{s} = \frac{-3mh^2\frac{\delta s}{s_0}}{s_0^3} - \frac{17c_0\mu_{avg}^2(2\frac{\delta\mu}{\mu_{avg}}-4\frac{\delta s}{s_0})}{16s_0^4}$$

Grouping the Terms

$$\mu_{avg}^2 = \frac{16smh^2}{17c_0} \quad \text{derived from Equation A.1.3}$$

Equation A.1.4 $\quad m\delta\ddot{s} - \frac{mh^2}{s_0^4}\delta s = -2\frac{mh^2}{\mu_{avg}s_0^3}\delta\mu$

Taking the Laplace Transform of the homogenous equation (Using S as the Laplace variable for clarity)

$$mS^2 - \frac{mh^2}{s_0^4} = 0$$

Equation A.1.5 $S = \pm\sqrt{\dfrac{h^2}{s_0^4}} = \pm\Omega$

Appendix A.2 Derivation of Poles for 16.62x Setups

Appendix A.2.1 Derivation of Poles for Stable 16.62x Setup
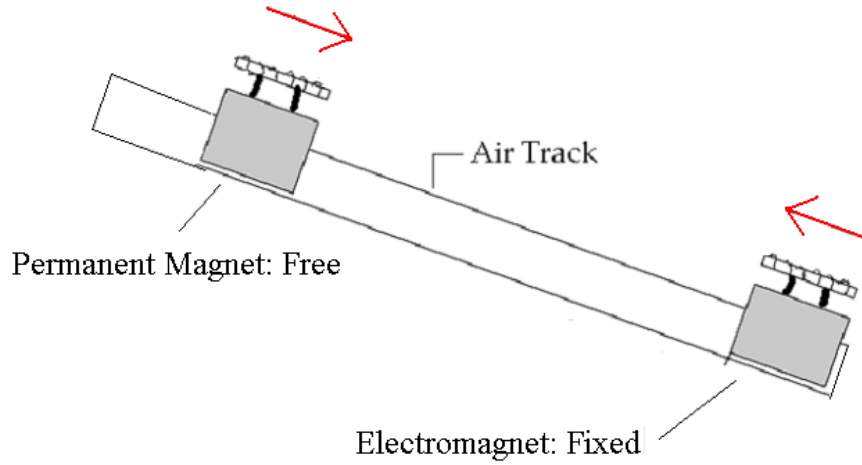
Figure A.2.1.1 16.62x Stable Setup

Force Balance

Assume the two vehicles have opposite magnetic moments, so $\mu \equiv \mu_A = -\mu_B$.

Equation A.2.1.1 $F_{EM} - F_{grav} = 0$

Equation A.2.1.2 $F_{EM} = \dfrac{c_0 \mu^2}{s^4}$ where $c_0 = \dfrac{3\mu_0}{2\pi}$

Equation A.2.1.3 $F_{grav} = mgSin(\theta)$

where m is the mass of the free magnet, g is gravitational acceleration, and θ is the angle of the track

$$m\ddot{s} = F_{EM} - F_{grav} = \frac{c_0 \mu^2}{s^4} - mgSin(\theta)$$

Add a perturbation

$$m(\ddot{s}_0 + \delta\ddot{s}) = \frac{c_0 (\mu_{avg} + \delta\mu)^2}{(s_0 + \delta s)^4} - mgSin(\theta)$$

$\ddot{s}_0 = 0$ because s_0 is the constant, steady-state displacement

$$m\delta\ddot{s} = \frac{c_0 \mu_{avg}^2 (1 + \dfrac{\delta\mu}{\mu_{avg}})^2}{s_0^4 (1 + \dfrac{\delta s}{s_0})^4} - mgSin(\theta)$$

Binomial Expansion $(1 + x)^n = 1 + nx +$ higher order terms for $|x| \ll 1$

$$m\delta\ddot{s} = \frac{c_0 \mu_{avg}^2 (1 + 2\dfrac{\delta\mu}{\mu_{avg}})(1 - 4\dfrac{\delta s}{s_0})}{s_0^4} - mgSin(\theta)$$

$$m\delta\ddot{s} = \frac{c_0 \mu_{avg}^2 (1 + 2\dfrac{\delta\mu}{\mu_{avg}} - 4\dfrac{\delta s}{s_0} - 8\dfrac{\delta\mu\delta s}{\mu_{avg} s_0})}{s_0^4} - mgSin(\theta)$$

Neglect Higher Order Terms

$$m\delta\ddot{s} = \frac{c_0 \mu_{avg}^2 (1 + 2\dfrac{\delta\mu}{\mu_{avg}} - 4\dfrac{\delta s}{s_0})}{s_0^4} - mgSin(\theta)$$

Cancel Force Balance Terms

In the steady state case, when $\ddot{s} \to 0$ (so that $s = s_0$, and $\mu = \mu_{avg}$):

$$F_{EM} - F_{grav} = \frac{c_0 \mu_{avg}^2}{s_0^4} - mgSin(\theta) = 0$$

so that the steady-state terms cancel in the equation of motion, leaving:

$$m\delta\ddot{s} = \frac{c_0 \mu_{avg}^2 (2\dfrac{\delta\mu}{\mu_{avg}} - 4\dfrac{\delta s}{s_0})}{s_0^4}$$

Grouping the Terms

Equation A.2.1.4 $m\delta\ddot{s} + \dfrac{4c_0 \mu_{avg}^2}{s_0^5} \delta s = \dfrac{2c_0 \mu_{avg}}{s_0^4} \delta\mu$

Taking the Laplace Transform of the homogeneous equation (Using S as the Laplace variable for clarity)

$$mS^2 + \frac{4c_0\mu_{avg}^2}{s_0^5} = 0$$

Equation A.2.1.5 $S = \pm\sqrt{\frac{4c_0\mu_{avg}^2}{ms_0^5}}i$

Appendix A.2.2 Derivation of Poles for Unstable 16.62x Setup
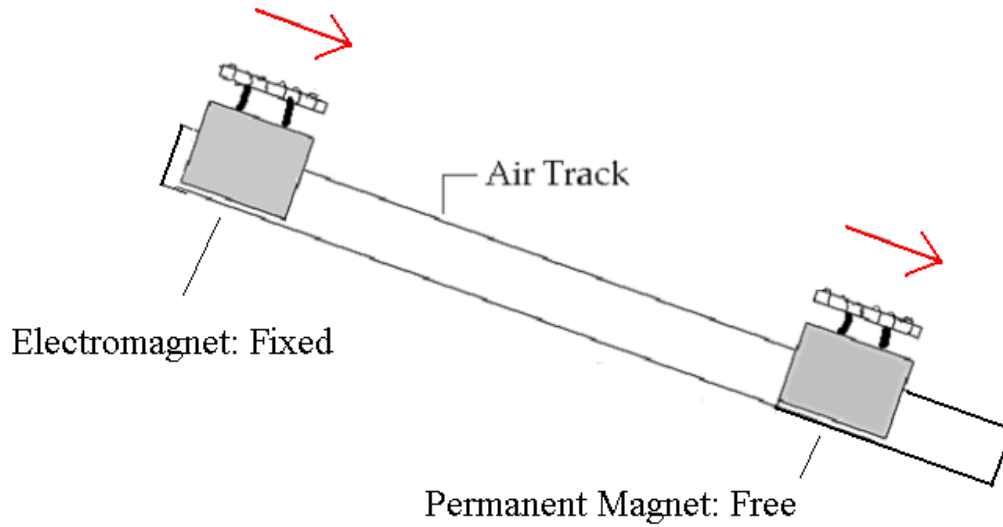
Figure A.2.2.1 16.62x Unstable Setup

Force Balance

Assume the two vehicles have equal magnetic moments, so $\mu \equiv \mu_A = \mu_B$.

Equation A.2.2.1 $F_{EM} = F_{grav}$

Equation A.2.2.2 $F_{EM} = \dfrac{c_0 \mu^2}{s^4}$ where $c_0 = \dfrac{3\mu_0}{2\pi}$

Equation A.2.2.3 $F_{grav} = mgSin(\theta)$

  where m is the mass of the free magnet, g is gravitational acceleration, and θ is the angle of the track

$$m\ddot{s} = F_{grav} - F_{EM} = mgSin(\theta) - \frac{c_0 \mu^2}{s^4}$$

Add a perturbation

$$m(\ddot{s}_0 + \delta\ddot{s}) = mgSin(\theta) - \frac{c_0 (\mu_{avg} + \delta\mu)^2}{(s_0 + \delta s)^4}$$

$\ddot{s}_0 = 0$ because s_0 is the constant, steady-state displacement

$$m\delta\ddot{s} = mgSin(\theta) - \frac{c_0 \mu_{avg}^2 (1 + \dfrac{d\mu}{\mu_{avg}})^2}{s_0^4 (1 + \dfrac{ds}{s_0})^4}$$

Binomial Expansion $(1+x)^n = 1 + nx +$ higher order terms for $|x| \ll 1$

$$m\delta\ddot{s} = mgSin(\theta) - \frac{c_0\mu_{avg}^2(1+2\frac{\delta\mu}{\mu_{avg}})(1-4\frac{\delta s}{s_0})}{s_0^4}$$

$$m\delta\ddot{s} = mgSin(\theta) - \frac{c_0\mu_{avg}^2(1+2\frac{\delta\mu}{\mu_{avg}}-4\frac{\delta s}{s_0}-8\frac{\delta\mu\delta s}{\mu_{avg} s_0})}{s_0^4}$$

Neglect Higher Order Terms

$$m\delta\ddot{s} = mgSin(\theta) - \frac{c_0\mu_{avg}^2(1+2\frac{\delta\mu}{\mu_{avg}}-4\frac{\delta s}{s_0})}{s_0^4}$$

Cancel Force Balance Terms

In the steady state case, when $\ddot{s} \to 0$ (so that $s = s_0$, and $\mu = \mu_{avg}$):

$$F_{EM} - F_{grav} = \frac{c_0\mu_{avg}^2}{s_0^4} - mgSin(\theta) = 0$$

so that the steady-state terms cancel in the equation of motion, leaving:

$$m\delta\ddot{s} = \frac{c_0\mu_{avg}^2(4\frac{\delta s}{s_0}-2\frac{\delta\mu}{\mu_{avg}})}{s_0^4}$$

Grouping the Terms

Equation A.2.4 $m\delta\ddot{s} - \frac{4c_0\mu_{avg}^2}{s_0^5}\delta s = -\frac{2c_0\mu_{avg}}{s_0^4}\delta\mu$

Taking the Laplace Transform of the homogenous equation (Using S as the Laplace variable for clarity)

$$mS^2 - \frac{4c_0\mu_{avg}^2}{s_0^5} = 0$$

Equation A.2.5 $S = \pm\sqrt{\dfrac{4c_0\mu_{avg}^2}{ms_0^5}}$

Appendix A.3 State Space Analysis

State Space Equation

Equation A.3.1
$$\begin{bmatrix} \dfrac{\delta \ddot{s}}{s_0} \\ \dfrac{\delta \dot{s}}{s_0} \end{bmatrix} = \begin{bmatrix} 0 & 1 \\ \Omega^2 & 0 \end{bmatrix} \begin{bmatrix} \dfrac{\delta s}{s_0} \\ \dfrac{\delta \dot{s}}{s_0} \end{bmatrix} + \begin{bmatrix} 0 \\ -2\Omega^2 \end{bmatrix} \dfrac{\delta \mu}{\mu_{avg}}$$

of form

$$\dot{x} = Ax + Bu$$

Want to minimize J, where J is a cost function.

Equation A.3.2
$$J = \int_0^\infty [x^T R_{xx} x + u^T R_{uu} u] dt$$

Equation A.3.3
$$u = -R_{uu}^{-1} B^T P x = -Fx$$

Equation A.3.4
$$R_{xx} + PA + A^T P - PBR_{uu}^{-1}B^T P = 0$$

Variable Definitions

$$R_{uu} = \rho \qquad R_{xx} = \begin{bmatrix} \lambda & 0 \\ 0 & 0 \end{bmatrix} \qquad P = \begin{bmatrix} P_{11} & P_{12} \\ P_{12} & P_{22} \end{bmatrix}$$

Plug into Equation D.3.4

$$\begin{bmatrix} 0 & 0 \\ 0 & 0 \end{bmatrix} = \begin{bmatrix} \lambda & 0 \\ 0 & 0 \end{bmatrix} + \begin{bmatrix} P_{11} & P_{12} \\ P_{12} & P_{22} \end{bmatrix}\begin{bmatrix} 0 & 1 \\ \Omega^2 & 0 \end{bmatrix} + \begin{bmatrix} 0 & \Omega^2 \\ 1 & 0 \end{bmatrix}\begin{bmatrix} P_{11} & P_{12} \\ P_{12} & P_{22} \end{bmatrix} - \begin{bmatrix} P_{11} & P_{12} \\ P_{12} & P_{22} \end{bmatrix}\begin{bmatrix} 0 \\ -2\Omega^2 \end{bmatrix}\frac{1}{\rho}\begin{bmatrix} 0 & 2\Omega^2 \end{bmatrix}\begin{bmatrix} P_{11} & P_{12} \\ P_{12} & P_{22} \end{bmatrix}$$

Three distinct equations result

Equation A.3.5
$$0 = \lambda + 2P_{12}\Omega^2 - 4\frac{\Omega^4}{\rho}P_{12}^2$$

Equation A.3.6
$$0 = P_{11} + P_{22}\Omega^2 - 4\frac{\Omega^4}{\rho}P_{12}P_{22}$$

Equation A.3.7
$$0 = 2P_{12} - 4\frac{\Omega^4}{\rho}P_{22}^2$$

Solve Equation A.3.5 for P_{12}

$$P_{12} = \frac{\rho}{4\Omega^2}\left(1 \pm \sqrt{1 + 4\frac{\lambda}{\rho}}\right)$$

Plug into Equation A.3.6 and solve for P_{22}

$$P_{22} = \pm\sqrt{\frac{\rho}{2\Omega^4}\frac{\rho}{4\Omega^2}\left(1 \pm \sqrt{1 + 4\frac{\lambda}{\rho}}\right)}$$

Both values must be positive to be real, therefore

$$P_{12} = \frac{\rho}{4\Omega^2}\left(1 + \sqrt{1 + 4\frac{\lambda}{\rho}}\right) \quad \text{and} \quad P_{22} = \sqrt{\frac{\rho^2}{8\Omega^6}\left(1 + \sqrt{1 + 4\frac{\lambda}{\rho}}\right)}$$

Solve Equation A.3.6 for P_{11}

$$P_{11} = \Omega^2\sqrt{\frac{\rho^2}{8\Omega^6}\left(1 + \sqrt{1 + 4\frac{\lambda}{\rho}}\right)}\sqrt{1 + 4\frac{\lambda}{\rho}}$$

From A.3.3

$$F = \frac{1}{\rho}\begin{bmatrix} 0 & -2\Omega^2 \end{bmatrix}\begin{bmatrix} P_{11} & P_{12} \\ P_{12} & P_{22} \end{bmatrix} = \frac{-2\Omega^2}{\rho}\begin{bmatrix} P_{12} & P_{22} \end{bmatrix}$$

if $\dfrac{\lambda}{\rho} \to 0$, $P_{12} \to \dfrac{\rho}{4\Omega^2}[2] = \dfrac{\rho}{2\Omega^2}$

$$P_{22} \to \frac{\rho}{2\Omega^3}$$

$$F = \frac{-2\Omega^2}{\rho}\begin{bmatrix} \frac{\rho}{2\Omega^2} & \frac{\rho}{2\Omega^3} \end{bmatrix} = -\frac{1}{\Omega}\begin{bmatrix} \Omega & 1 \end{bmatrix}$$

$$\dot{x} = Ax + Bu = Ax - BFx = \begin{bmatrix} A - BF \end{bmatrix}x = A_{CL}x$$

where $A_{CL} = \begin{bmatrix} 0 & 1 \\ \Omega^2 & 0 \end{bmatrix} - \begin{bmatrix} 0 \\ -2\Omega^2 \end{bmatrix}\frac{-1}{\Omega}\begin{bmatrix} \Omega & 1 \end{bmatrix} = \begin{bmatrix} 0 & 1 \\ -\Omega^2 & -2\Omega \end{bmatrix}$

solutions of $|SI - A_{CL}| = \begin{vmatrix} S & -1 \\ \Omega^2 & S + 2\Omega \end{vmatrix}$

yield $(S + \Omega) = 0$, two closed loop poles at -Ω.

if $\dfrac{\lambda}{\rho} \gg 1$, $P_{12} \to \dfrac{\rho}{4\Omega^2}[2]\dfrac{\lambda}{\rho} = \dfrac{\rho}{2\Omega^2}\dfrac{\lambda}{\rho}$

$$P_{22} \to \frac{\rho}{2\Omega^3}\frac{\lambda}{\rho}$$

$$F = \frac{-2\Omega^2}{\rho}\begin{bmatrix} P_{12} & P_{22} \end{bmatrix} = \begin{bmatrix} -\frac{1}{2}\left(1+\sqrt{1+4\frac{\lambda}{\rho}}\right) & -\frac{\sqrt{2}}{2\Omega}\sqrt{1+\sqrt{1+4\frac{\lambda}{\rho}}} \end{bmatrix}$$

$$\dot{x} = Ax + Bu = Ax - BFx = \begin{bmatrix} A - BF \end{bmatrix}x = A_{CL}x$$

where

$$A_{CL} = \begin{bmatrix} 0 & 1 \\ \Omega^2 & 0 \end{bmatrix} - \begin{bmatrix} 0 \\ -2\Omega^2 \end{bmatrix}\begin{bmatrix} -\frac{1}{2}\left(1+\sqrt{1+4\frac{\lambda}{\rho}}\right) & -\frac{\sqrt{2}}{2\Omega}\sqrt{1+\sqrt{1+4\frac{\lambda}{\rho}}} \end{bmatrix} = \begin{bmatrix} 0 & 1 \\ -\sqrt{1+4\frac{\lambda}{\rho}} & -\Omega\sqrt{2}\sqrt{1+\sqrt{1+4\frac{\lambda}{\rho}}} \end{bmatrix}$$

solutions of $\quad \left| SI - A_{CL} \right| = \begin{bmatrix} S & -1 \\ \sqrt{1+4\frac{\lambda}{\rho}} & S+\Omega\sqrt{2}\sqrt{1+\sqrt{1+4\frac{\lambda}{\rho}}} \end{bmatrix}$

yield two closed loop poles at:

$$s = \Omega \sqrt[4]{\frac{\lambda}{\rho}}(-1 \pm i)$$
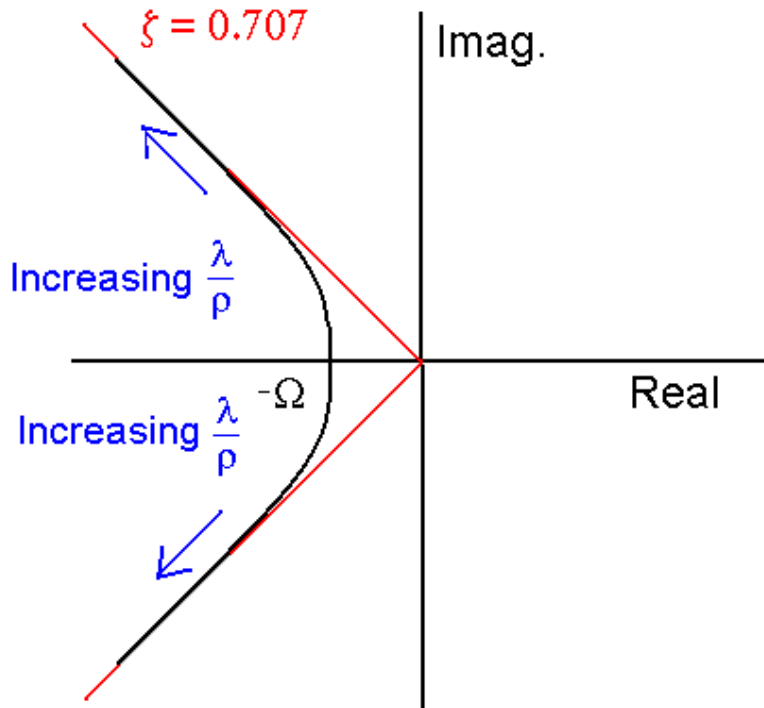
Figure A.3.1 Plot of Position of Closed Loop Poles